HHS Public Access

Author manuscript

Dev Neurobiol. Author manuscript; available in PMC 2020 May 01.

Published in final edited form as:

Dev Neurobiol. 2019 May ; 79(5): 479–496. doi:10.1002/dneu.22676.

Loss of neurogenesis in aging *Hydra*

Szymon Tomczyk[1,2], **Wanda Buzgariu**[1,2], **Chrystelle Perruchoud**[1,2], **Kathleen Fisher**[3], **Steven Austad**[3], **Brigitte Galliot**[1,2,°]

[1]Department of Genetics and Evolution, Faculty of Sciences, University of Geneva, Switzerland [2]iGE3 -Institute for Genomics and Genetics in Geneva, Switzerland [3]Department of Biology, University of Alabama at Birmingham, USA

Abstract

In *Hydra* the nervous system is composed of neurons and mechano-sensory cells that differentiate from interstitial stem cells, which also provide gland cells and germ cells. The adult nervous system is actively maintained through continuous *de novo* neurogenesis that occurs at two distinct paces, slow in intact animals and fast in regenerating ones. Surprisingly *Hydra vulgaris* survive the elimination of cycling interstitial cells and the subsequent loss of neurogenesis if force-fed. By contrast, *H. oligactis* animals exposed to cold temperature undergo gametogenesis and a concomitant progressive loss of neurogenesis. In the cold-sensitive strain *Ho_CS*, this loss irreversibly leads to aging and animal death. Within four weeks, *Ho_CS* animals lose their contractility, feeding response and reaction to light. Meanwhile, two positive regulators of neurogenesis, the homeoprotein prdl-a and the neuropeptide *Hym-355*, are no longer expressed, while the “old” RFamide-expressing neurons persist. A comparative transcriptomic analysis performed in cold-sensitive and cold-resistant strains confirms the down-regulation of classical neuronal markers during aging but also shows the up-regulation of putative regulators of neurotransmission and neurogenesis such as *AHR, FGFR, FoxJ3, Fral2, Jagged, Meis1, Notch, Otx1, TCF15*. The switch of *Fral2* expression from neurons to germ cells suggests that in aging animals, the neurogenic program active in interstitial stem cells is re-routed to germ cells, preventing *de novo* neurogenesis and impacting animal survival.

Keywords

Hydra nervous system; interstitial stem cells; adult *de novo* neurogenesis; gametogenesis; aging; homeoprotein prdl-a; neuropeptide Hym-355; evolution of neurogenesis

Introduction

The freshwater hydrozoan *Hydra* polyp (Fig. 1A) belongs to Cnidaria, a phylum that includes anthozoans (sea anemones, corals) and medusozoans (jellyfish) (Collins et al., 2006). Their common ancestor arose prior to the common ancestor of bilaterians (Fig. 1B) and Cnidaria together with Bilateria are eumetazoans, i.e. animals equipped with a nervous

° Corresponding author: brigitte.galliot@unige.ch.

system and epithelial layers, the internal one forming a gut and the external one an epidermis (Fig. 1C). Among cnidarians, the hydrozoan *Hydra* polyp is well known for its amazing capacity to regenerate within few days any missing body part after amputation including its complete nervous system. In fact, the central body column of the animal is populated all along its life with multipotent interstitial stem cells (ISCs) that beside germ cells and gland cells produce all cells of the nervous system, as well as epithelial stem cells in the epidermis (eESCs) and the gastrodermis (gESCs) (Buzgariu et al, 2014). ISCs produce neuronal precursors that migrate towards the extremities of the animal where they differentiate to replace cells that die or get sloughed off (Bode et al., 1973; Fujisawa, 1989; Teragawa and Bode, 1995; Technau and Holstein, 1996). As a consequence, the *Hydra* nervous system is much denser at the apical and basal poles. This process that takes several weeks in homeostatic conditions is completed within several days when the animals regenerate its apical or basal extremity (Wenger et al. 2016).

Cnidarian neurons that form neurites but no typical axons, therefore often named “nerve cells”, can be sensory, sensory-motor bipolar and multipolar also named ganglia neurons (Fig. 1D). These ganglia neurons function as interneurons that form in some species a well visible nerve ring at the base of the tentacles, often recognized as a simple form of cephalisation (Koizumi, 2007). Beside nerve cells, a large pool of mechano-sensory cells named cnidocytes or nematocytes contribute to the feeding and defense behaviors, as equipped with a cnidocil that, upon stimulation, triggers the discharge of the cnidocyst, a phylum-specific organelle that functions as a weapon full of venom (Tardent, 1995). The two main cell lineages that form the *Hydra* nervous system are quite different at the quantitative level (Bode et al., 1973; David, 1973), the neurons being rather rare (3% of all cell types) and functional for several weeks while the abundant nematocytes (35%) are “single-usage”, replaced once they have discharged their venom capsule.

Cnidarian and bilaterian nervous systems follow the same principles of synaptic conduction and chemical neurotransmission (Anderson and Spencer, 1989; Kass-Simon and Pierobon, 2007), even though cnidarian neurons heavily make use of peptides with peptide-gated ion channels as receptors (Grimmelikhuijzen and Westfall, 1995; Grunder and Assmann, 2015). The pool of transcription factors involved in bilaterian neurogenesis are largely expressed in cnidarian nervous systems (Grens et al., 1995; Gauchat et al., 1998, 2004; Miljkovic-Licina et al., 2004, 2007; Galliot et al., 2009; Marlow et al., 2009; Galliot and Quiquand, 2011), suggesting a common origin between cnidarian and bilaterian nervous systems. Still, some neuropeptides impact neuronal differentiation, positively in case of Hym-355 (Takahashi et al., 2000).

Another amazing feature of *Hydra* is its ability to survive short antimitotic treatments (hydroxyurea, colchicine) that eliminate the fast cycling ISCs but leave intact the two epithelial stem cell populations (Campbell, 1976; Marcum and Campbell, 1978; Marcum et al., 1980). Upon such treatments, *de novo* neurogenesis is suppressed and animals progressively loose all their nerve cells. In few weeks the cell lineages that derive from ISCs are depleted making the animal “nerve-free” (Sacks and Davis, 1979). Surprisingly such nerve-free animals can survive months and years if manually force-fed and their developmental capacities are not impaired, meaning that animals only equipped with two

epithelial layers still regenerate and, if heavily fed, bud. A recent transcriptomic analysis showed that these epithelial cells (Fig. 1E) actually up-regulate a large number of genes, including genes normally predominantly expressed in ISCs or their derivatives (Wenger et al., 2016). The functional consequences of these genetic modulations have not been explored yet, but this result highlights an epithelial plasticity at the transcriptional level when neurogenesis fails.

Three main studies performed over the past 70 years indicate that *Hv* polyps have an extremely long lifespan or might even escape aging completely (Brien, 1953; Martínez, 1998; Schaible et al., 2015). The dynamic maintenance of the three populations of stem cells is necessary for slow aging and more specifically the stock of ISCs for maintaining a continuous neurogenesis in adult animals. How *Hydra* polyps maintain over long periods of time stocks of adult stem cells without any DNA-damage or cellular alteration is poorly understood. In a distinct species named *H. oligactis* (Fig. 1A), aging rapidly follows the induction of gametogenesis, which is obtained by transferring the animals from room temperature (RT) to 10°C (Brien, 1953). After few weeks, the intense production of gametes leads to the depletion of the somatic populations derived from ISCs, and animals cannot maintain their fitness (Yoshida et al., 2006).

More recently, we characterized two distinct *H. oligactis* strains that exhibit different responses to cold-induced gametogenesis; one that undergoes aging (*Ho_CS)* and another that resists to aging (*Ho_CR)* (Tomczyk et al., 2017). *Ho_CS* animals exhibit the typical aging phenotype reported by Brien (1953) and Yoshida et al. (2006), we also noted the disorganization of the apical nervous system (Tomczyk et al., 2015). At the epithelial level, we identified two main differences between aging-sensitive and aging-resistant animals, (i) the inducibility of the autophagy flux that appears deficient in *Ho_CS,* and (ii) the self-renewal of ESCs that progressively and irreversibly decreases in aging animals (Tomczyk et al., 2017). The importance of autophagy for stem cell homeostasis was demonstrated in multiple cell types as recently reviewed by (Boya et al., 2018). Autophagy also plays a key role in the maturation and survival of adult-generated neurons but the mechanisms remain unknown (Xi et al., 2016). With this study our aim was to characterize at the behavioral, cellular and molecular levels the degeneration of the nervous system in aging *H. oligactis.*

Materials & methods

Hydra culture and induction of aging

Strains of *Hydra vulgaris* (*Hv_Basel)* or *Hydra oligactis,* identified as Cold Sensitive (*Ho_CS*) and Cold Resistant (*Ho_CR)* were mass-cultured in Hydra Medium (HM: 1 mM NaCl, 1 mM $CaCl_2$, 0.1 mM KCl, 0.1 mM $MgSO_4$, 1 mM Tris-HCl pH 7.6) and fed twice a week with freshly hatched brine shrimps. To induce aging *Ho_CS* and *Ho_CR* animals were transferred from 18°C ± 0.5°C, the standard temperature for *Hydra* culture, to incubators at 10°C ± 0.3°C. For animals maintained at 10°C all washes were done with pre-cooled HM (10°C) and transferred to sterile cold culture dishes. For transcriptomic analyses, animals from the *Hv_Jussy, Hv_sf1, Hv_AEP* strains were used as reported in Wenger et al. (2016).

Behavioral and morphometric analyses

For touch responsiveness, animals were stimulated with tweezers in the peduncle region and observed under the binocular and the time between tweezer stimulation and contraction was noted for each *Ho_CS* animal maintained either at 18°C or at 10°C for 35 days. For light response, 15 polyps maintained at 18°C or 10°C in dim light were allowed to fully extend in a darkened room, then exposed to a LED light source placed 19 cm above the animals to record body column contractions (at least 25% of their length). The latency period corresponds to the time between initial light exposure and the observed first contraction (5 minutes at most). For prey capture, 15 polyps per condition were placed in a 24-well plate pre-filled with 1 ml HM containing *Artemia*. After 15 seconds the animals were transferred to HM-containing wells, the number of captured *Artemia* was recorded and normalized by tentacle number. The variations in hypostome size were measured by manually delimiting the hypostome area on the images taken with Leica DM5500. The delimited surface was measured with Fiji.

Immunofluorescence (IF) on macerated tissues and on whole mounts

Procedures were as described in (Wenger et al. 2016). Briefly, for IF on cells *Hydra,* tissues were macerated according to (David, 1973). The cell suspension was spread on positively charged Superfrost Plus slides (Thermo Scientific) and dried for two days at RT, then washed in PBS, blocked with PBS, 2% BSA, 0.1% Triton-X100 for 2 hours, and incubated with the **anti a-tubulin** antibody overnight at 4°C. After washes in PBSTw (PBS, 0.1% Tween-20), cells were incubated in the anti-rabbit AlexaFluor-488 antibody (1:600, Thermofisher), counterstained with DAPI and imaged on a Leica SP8 confocal microscope. For IF on whole mounts, animals were briefly relaxed in urethane 2% (60 seconds), then fixed in 4% paraformaldehyde (PFA) prepared in HM when immunodetected with the rabbit polyclonal serum raised against the **RFamide** neuropeptide (Grimmelikhuijzen, 1985; Wenger et al. 2016). When immunodetected with the rabbit polyclonal serum raised against the **prdl-a** homeoprotein (Gauchat et al., 1998), animals were fixed in Lavdowsky fixative (50% ethanol, 3.7% formaldehyde, 4% acetic acid) for one hour at 37°C, washed several times in PBS, and incubated in 2N HCl for 30 min for DNA denaturation. Then, whatever the fixation condition, animals were washed in PBS, blocked in PBS, 2% BSA, 0.1% Triton-X100 for 2 hours, incubated overnight at 4°C with the primary antibody (1:1000), washed in PBSTw and incubated with the appropriate anti-rabbit AlexaFluor antibody (AlexaFluor-488 or AlexaFluor-555, 1:600, Thermofisher). The samples were finally washed in PBSTw, DAPI stained and pictured on a Leica SP8 or Zeiss LSM700 confocal microscope.

BrdU detection and whole mount In situ hybridization (WM-ISH)

Animals were incubated in 5 mM **5'-bromodeoxyuridine (BrdU)** for four hours, washed and maintained in HM for two days, and fixed in 4% PFA/HM for four hours then in ethanol overnight at −20°C. The transcripts were detected with a digoxygenin (DIG)-labelled riboprobes specific to *Hym355, prdl-a, TCF15* or *Fral2* and the samples were processed for WM-ISH as in (Bode et al., 2008). In case of *H. oligactis* animals, the WM-ISH procedure was shortened at several steps to account for their higher frailty: proteinase K digestion was 8 min and 10 min for animals maintained at 10°C and 18°C respectively, the 80°C pre-heat

step was 20 min, the probe hybridization step 16 hours and the post-hybridization MAB washes 6× 15 min. Whatever the species, the hybridized riboprobes were similarly detected by NBT-BCIP staining, the samples were then post-fixed in 3.7% FA for 30 minutes, washed for 15 min in methanol and 3× 10 min in PBSTr (PBS, 0.1% Triton X-100). Next, the samples were treated with 2N HCl for 30 min, washed in PBST several times over 15 min, incubated overnight at 4°C with the **anti-BrdU** antibody (1:20, Roche), washed 4× 10 min in PBS and incubated in the anti-mouse Alexa 488-coupled secondary antibody (1:500, Molecular Probes) for four hours at RT. Then animals were labeled with DAPI for 10 minutes, washed in PBS (4× 10 min), 5 min in H2O, mounted in Mowiol and imaged on a Leica D5500 microscope equipped with a color DMC2900 and a monochromatic DFC9000 camera.

BrdU and prdl-a double immuno-labeling

Intact *H. vulgaris* were incubated with 5 mM BrdU for four hours and either amputated at mid-gastric level and let to regenerate for four days, or washed and maintained intact in HM. At the indicated time, the animals were fixed for one hour at 37°C in Lavdowsky “minus” (50% ethanol, 3.7% FA), washed several times in PBS, treated with 2N HCl for 30 min and washed again in PBS. After one hour incubation in 2% BSA, PBS, the samples were incubated overnight with the **anti-BrdU** (1:20, Roche) and **anti-prdl_a** (1:1000, Gauchat 1998) antibodies, washed 4×10 min in PBS, incubated with the anti-mouse Alexa 488 and anti-rabbit Alexa 555 antibodies (1:500, Molecular Probes), washed again 4× 10 min in PBS, incubated for 10 min in DAPI (1 µg/ml in PBS), washed 2× 5 min in PBS, briefly in water and mounted in Mowiol. Imaging was performed with a LSM700 Zeiss confocal microscope. For quantification of interstitial cell proliferation in *Ho_CS,* animals were exposed to BrdU for 24 hours at indicated time points of the aging process. At the end of the treatment animals were macerated as in (David, 1973) and immunodetected with the anti-BrdU antibody as described above. The BrdU+ nuclei were counted manually to establish the BrdU-labeling index.

Transcriptomic analyses

The quantitative RNA-sequencing analysis (qRNA-seq) performed on *Ho_CS* and *Ho_CR* animals maintained either at 18°C or at 10°C is detailed in (Tomczyk et al., 2017). The qRNA-seq performed either on *Hv_Jussy* animals sliced at five distinct positions along the body axis (Supplementary Figure-S1), or on *Hv_sf1* animals exposed to drugs (hydroxyurea, colchicine) or to heat-shock, or on transgenic *Hv_AEP* animals expressing GFP in one or the other stem cell populations is reported in (Wenger et al., 2016). Values that were obtained in biological triplicates for each condition are available in Table-S1 from Wenger et al. (2016). For heatmap representations, each value corresponds to the average number of reads obtained at indicated time points. Orthologous relationships between *Hv_sf1, Ho_CR* and *Ho_CS* sequences were assigned manually. GraphPad Prism 7 was used to generate the scatterplots of fold change differences between *Ho* and *Hv* RNA-seq values and the regression analysis. Sequences and RNA-seq profiles are publicly available, for *H. vulgaris* at https://Hydratlas.unige.ch, for *Ho_CS* and *Ho_CR* at http://129.194.56.90/blast/.

Results

Sustained *de novo* neurogenesis in long lived *H. vulgaris*

To demonstrate the *de novo* production of neurons in homeostatic and regenerating non-aging animals we used two established markers for neuronal progenitors and nerve cells, the homeoprotein prdl-a and the neuropeptide *Hym-355* respectively. Both prdl-a and Hym-355 are involved in the control of neurogenesis, prdl-a in the production of apical neuronal progenitors (Gauchat et al., 1998), Hym-355 in the neuronal differentiation of interstitial progenitors (Takahashi et al., 2000). In homeostatic conditions, both *prdl-a* transcripts and the prdl-a protein are predominantly expressed in apical interstitial progenitors (Fig. 2A, 2D) while *Hym-355* is expressed in apical and basal subpopulations of neurons, and to a lower extent in the body column (Fig. 2A, 2B). The animals fixed four days after a short exposure to BrdU do not show any BrdU+ cells that express *Hym-355* (Fig. 2B). Under homeostatic conditions, the number of neurons produced each day is rather low as *de novo* neurogenesis is slow (Hager and David, 1997), explaining why BrdU/*Hym-355* positive neurons cannot be detected in this condition.

During regeneration, the dense nervous systems in the head and peduncle are re-established, in few days to maintain the animal fitness. Immediately after amputation, neuronal progenitors migrate toward the wound to contribute to the regeneration of the nervous system in the newly formed structure. In the regenerating tips the expression of *prdl-a* and *Hym-355* is re-established with different kinetics: *prdl-a* shows a dual regulation with a first immediate but transient expression in gastrodermal cells (Gauchat et al., 1998), followed by an up-regulation in interstitial progenitors of the head-regenerating tip from 16 hours post-amputation (hpa) (Fig. 2C). By contrast, *Hym-355* starts to be up-regulated later, detected in both the head-and foot-regenerating tips after 24 hpa (Fig. 2C). To visualize the induction of neurogenesis in regenerating animals, we coupled prdl-a immunodetection to BrdU labeling: *H. vulgaris* animals bisected at mid-gastric position were immediately exposed to BrdU for four hours, then left to regenerate for four days and fixed for immunodetection. In such conditions, we noticed a high increase in the number of $BrdU^+$/prdl-a^+ nuclei when compared to non-bisected animals (Fig. 2D), reflecting the anticipated fast neurogenesis process.

These two types of *de novo* neurogenesis, slow in intact animals and fast in regenerating ones, do not seem to be altered in animals kept for several years as these animals regenerate well the missing structures and maintain their active behaviors, i.e. feeding, contracting, walking (Brien, 1953; Martínez, 1998). By contrast, *H. oligactis* animals exposed to cold temperature, a condition that induces gametogenesis, rapidly loose their fitness and the ability to maintain a dynamic neurogenesis (Brien, 1953; Yoshida et al., 2006; Tomczyk et al., 2015) (Fig. 3A).

Aging *H. oligactis* lose their contractility and feeding capacity

To test the impact of aging on the various functions of the nervous system, we compared the behaviors of aging and non-aging animals exposed to mechanical stimulus, light or food. We first tested the contractility induced by a mechanical stimulus, i.e. a pinch in the peduncle

region (Fig. 3B). We found that while *Ho_CS* animals maintained at 18°C contract within two seconds, *Ho_CS* animals taken 35 days after transfer to 10°C show a much slower reaction time of 10 seconds (see supplementary movies). We also measured at regular time-points over a 30 days period after transfer to 10°C, the contraction latency in response to light (Fig. 3C). We recorded an increase in the contraction latency, from 40 to 100 seconds in *Ho_CS* animals while the initial value (60 seconds) remained stable in *Ho_CR* animals exposed to cold for the same period of time (Fig. 3C). The difference between the two strains was already visible at day-14 after the temperature switch.

The feeding behavior in *Hydra* is characterized by the capture of preys on the tentacles, the subsequent opening of the mouth and the coordinated movement of the tentacles to favor the ingestion of the preys through the mouth. This complex behavior is triggered by reduced glutathione release from the captured prey (Loomis, 1955; Grosvenor et al., 1996; Pierobon, 2015). Here animals were individually exposed to preys, i.e. swimming *Artemias*, for 15 seconds and the number of preys fixed on the tentacles was counted. This test that was performed at various time points after transfer to 10°C, showed a continuous decline in the ability to fix preys in *Ho_CS* animals, already visible at day-14 post transfer, but not in *Ho_CR* ones (Fig. 3D). After 30 days, a single prey was fixed on average on tentacles of *Ho_CS* animals versus six in *Ho_CR* animals. This decline reflects the inability of the animals to produce functional nematocytes that are normally abundant along the tentacles. After five to six weeks at 10°C, prey capture becomes impossible for *Ho_CS* animals as their head structures are heavily degenerated. These results show that both the contractility in response to light and the capacity to capture preys start to decline within 14 days after transfer to cold in *Ho_CS* but not in *Ho_CR*, progressively decreasing over the following weeks. This indicates that deficiencies in both neurogenesis and nematogenesis precede the morphological changes that appear at day-30.

Degeneration of the nervous system in aging *H. oligactis*

To investigate the nervous systems of the animals that show a decline of their behavioral functions, we analyzed the nerve cell density along the animal body, first by monitoring the distribution of the *Hym*-355 expressing neurons in *Ho_CS* animals undergoing aging. At 18°C, *Hym-355* neurons distribute in the apical and basal regions as well as along the body column in *Ho_CS* animals (Fig. 4A). In *H. vulgaris Hym-355* was described as predominantly expressed at the extremities, with only a low number of *Hym-355* neurons present in the body column (Takahashi et al., 2000). In *H. oligactis* as in *H. vulgaris, Hym-355* expression is restricted to nerve cells however *Hym-355* neurons are also numerous along the body axis, indicating species-specific variations. After one month at 10°C, we observed a severe loss of *Hym-355+* nerve cells, which are no longer detected after 41 days (Fig. 4A).

In parallel, we detected RFamide expressing neurons in *Ho_CS* and *Ho_CR* animals maintained at 18°C or at 10°C (Fig. 4B). RFamides are neuropeptides widely expressed in mature nerve cells along the body axis and at the extremities, highlighting the higher density of the nervous system at the apex and along the peduncle (Grimmelikhuijzen, 1985). As a low fraction of *Ho_CS* and *Ho_CR* animals do not undergo gametogenesis after transfer to

cold, we used sexual and asexual animals maintained for 36 days at 10°C to discriminate between the effects of cold stress versus gametogenesis and aging on the nervous system. We noted an obvious lower density of RFamide$^+$ nerve cells in the upper part of the body column in sexual *Ho_CS* animals, well visible in the region directly below the head. We noted the persistence of "old" RFamide$^+$ neurons at the apical extremity as well as in the peduncle region although the nerve net appears disorganized (Fig. 4B). In contrast, *Ho_CR* animals, sexual or asexual, maintained at 10°C for 36 days exhibit a nervous system that is not modified in terms of density or organization. Both neuronal markers, *Hym-355* and prdl-a, point to a clear degeneration of the nervous system in sexual *Ho_CS* animals maintained for weeks at 10°C.

Loss of *de novo* neurogenesis in aging *Hydra oligactis*

The observed loss of RFamide and *Hym-355* neurons could have various causes: (i) a loss of ISC proliferation necessary to replenish the stock of nerve cells, (ii) a disrupted differentiation of neuronal progenitors or (iii) a poor survival of the newly differentiated neurons. After transfer to 10°C both *Ho_CS* and *Ho_CR* exhibit a decrease in body size due to the change in the feeding rhythm, from four feedings per week at 18°C to two feedings at 10°C. However in *Ho_CS* animals this size decrease strongly affects the head structures that become three fold smaller within 35 days (Fig. 5A). As a consequence of the massive production of gametes, the proliferation of somatic interstitial cells measured after a 24 hours BrdU pulse drops to reach a minimal value after 32 days at 10°C, leading to a severe depletion of the stock of somatic ISCs as previously reported (Yoshida et al., 2006; Tomczyk et al., 2017). However, the rare somatic ISCs that survive readily cycle at later time-points (Fig. 5B).

To visualize the neuronal progenitors in *Ho_CS* animals taken at 44 or 45 days after transfer to cold, we detected the cells expressing *prdl-a* either by *in* situ hybridization (Fig. 5C) or by immunodetection with the antibody raised against *Hydra* prdl-a (Fig. 5D).

At 18°C *prdl-a* is predominantly expressed in neuronal progenitors located in the apical region, a pattern also observed in *Ho_CR* animals maintained at 10°C for 45 days (Fig. 5C). By contrast, *Ho_CS* animals maintained at 10°C for 45 days have very few apical cells expressing *prdl-a*, while some ectopic patches of non-neuronal *prdl-a* cells can be found in the body column. As anticipated, prdl-a protein in *Ho_CR* and *Ho_CS* animals maintained at 18°C is predominantly apical and nuclear (Fig. 5D, arrowheads), a pattern that remains stable in *Ho_CR* maintained at 10°C for 44 days. By contrast, in aging *Ho_CS* we observed a drastic decrease in the number of prdl-a$^+$ cells, likely reflecting a decrease in the number of neuronal precursors. The loss of apical prdl-a$^+$ cells suggests that the deterioration of the nervous system in aging *Ho_CS* is predominantly caused by the lack of *de novo* homeostatic neurogenesis, responsible for the insufficient renewal of the apical nervous system.

Aging-induced modulations of genes potentially involved in neurogenesis and neurotransmission

To further characterize the changes that occur in the nervous system of aging *Hydra,* we analyzed by quantitative RNA-seq (qRNA-seq) the expression of genes potentially

associated with neurogenesis (195) and neurotransmission (377), as previously annotated by Wenger et al. (2016). We retrieved the expression levels of these genes in *Ho_CS* and *Ho_CR* animals maintained at 10°C for 14 days, 26 days, 32 days, 35 days and 45 days (only *Ho_CS*) as previously reported (Tomczyk et al., 2017). Concerning the three *RFamide* genes (Hansen et al., 2000), *RFamide A* and *RFamide B* show very similar profiles in the two strains except an up-regulation of *RFamideA* in *Ho_CS* at 45 days (Fig. 6A). The persistence of the *RFamideA* transcripts in *Ho_CS* can be linked to their presumptive upregulation in the persisting neurons and/or to their ectopic expression in non-neuronal cell types. *RFamide C*, which is no longer expressed after 25 days at 10°C in *Ho_CR*, exhibits a burst of expression at day-25 in *Ho_CS* to become undetectable at day-45. Concerning *prdl-a,* we found its expression seemingly identical between *Ho_CS* and *Ho_CR* animals, a result compatible with the patterns detected by *in situ* hybridization (Fig. 6A).

To get a more global view of the modulations affecting the neurogenesis and neurotransmission genes, we produced heatmaps comparing gene expression levels in each strain (Fig. 6B–G). Among the 195 genes potentially associated with neurogenesis, we found 67 genes that are differently modulated in *Ho_CS* and *Ho_CR*, with 27 genes up-regulated in *Ho_CS* but not in *Ho_CR* (Fig. 6B), and 40 genes up-regulated in *Ho_CR* but not in *Ho_CS* (Fig. 6E). The former group that includes *Dlx, Dlx1, ELAV-A, ETS1, Fral2, Gli3, KLF8, Meis1, Otx1, Otx2B-1, PUM2, Sox123, TCF15* (Fig. 6B) might correspond to genes up-regulated in the remaining epithelial cells after the loss of the interstitial lineage, and/or to genes linked to the persisting gametogenesis in *Ho_CS*. The second group likely includes genes involved in the wave of *de novo* neurogenesis that follows gametogenesis in *Ho_CR* but not in *Ho_CS* (Fig. 6C). Among these 40 genes up-regulated in *Ho_CR*, one finds genes associated with interstitial stemness like *Myc-1, Pax-A, ZNF845* or *Nanos2* (Mochizuki et al., 2000; Hobmayer et al., 2012; Wenger et al., 2016). Loss of sustained expression of these genes in *Ho_CS* likely corresponds to the definitive loss of ISCs and progenitors. Interestingly *LMX1A*, which is up-regulated in epithelial cells of HU-treated animals (Wenger et al., 2016) is found in this category, suggesting that ESCs in aging *Ho_CS* are not able to up-regulate *LMX1A* in response to the loss of neurogenesis.

Among the 377 genes associated with neurotransmission, we found 114 genes with expression profiles differently modulated in *Ho_CS* and *Ho_CR*. We first identified 24 and 37 genes up-regulated at late time points in *Ho_CS* but not in *Ho_CR* where a large number show a transient down-regulation at day 14 (Fig. 6D, 6E). This group contains several genes that encode ubiquitin specific peptidases (Usp), which play important roles in the development and the physiology of bilaterian nervous systems as well as in neurodegenerative diseases (Baptista et al., 2012). As an example, Usp8 is implicated in the clearance of protein aggregates (Alexopoulou et al., 2016) and might in *Ho_CS* be involved in the response of old persisting neurons to the proteomic stress. Another group contains 41 genes similarly down-regulated in response to cold exposure in both *Ho_CS* and *Ho_CR*, possibly not linked to the aging process (Fig. 6F). Finally, 11 genes are maintained at high levels in *Ho_CR* but not in *Ho_CS* (Fig. 6G), likely reflecting the regeneration of a functional nervous system in *Ho_CR* but not in *Ho_CS* animals.

Impact of the loss of neurogenesis in HU-treated *H. vulgaris* and in aging *Ho_CS*

In *Hydra* the loss of neurogenesis can easily be achieved with anti-proliferative treatments such as hydroxyurea (HU) or colchicine. Such treatment in *Ho_CS* animals maintained at 18°C, so in the absence of gametogenesis, also leads to an aging phenotype (Tomczyk et al., 2017). This scenario resembles the aging process induced by gametogenesis in *Ho_CS* where the depletion of somatic interstitial progenitors leads to the disorganization of the nervous system. To investigate a possible similarity on the genetic level we compared the transcriptomic data obtained in *Ho_CS* and *Ho_CR* maintained at 10°C (Tomczyk et al., 2017) to those obtained in HU-treated *H. vulgaris (Hv_sf1)* (Wenger et al., 2016). In each context we retrieved the number of reads for the neurogenesis and neurotransmission associated genes in two conditions, at 18°C and 10°C day-35 for *Ho_CS* and *Ho_CR* animals (Fig. 7A), in untreated and HU-treated *Hv_sf1* animals taken seven days after HU exposure (Fig. 7B). We calculated the log2 fold change (FC) for all selected genes (Fig. 7C) and produced a scatterplot representation of the changes in gene expression between *Hv_sf1* post-HU and *Ho_CS* or *Ho_CR* maintained at 10°C.

That way, we identified a series of genes strongly up-regulated in *Ho_CS* but not in *Ho_CR*. Among the genes up-regulated at least four fold in *Ho_CS*, we identified *ADORA2A-L, CC2D2A, CHRNA9, DDCL2, EGCase, GPR139, GPR157, NCAM1, STK33* as neurotransmission genes (Fig. 7D) and *AHR, Fral2, FGFR, FoxJ3, Jagged, Meis1, Notch, Otx1, TCF15* as neurogenesis genes (Fig. 7E, 7F). These putative neurogenesis genes are up-regulated at least two-fold in 35 days old *Ho_CS* animals (blue numbers), much higher than in *Ho_CR* maintained at 10°C for 35 days (black numbers) where their expression is stable or mildly up-regulated (*Otx1*, *FGFR*) except in case of *TCF15* that is up-regulated 2.5 fold. Their up-regulation in *Ho_CS* also contrasts with the stable expression noted in *Hv_sf1* having lost their ISCs upon HU treatment (red numbers) except *Fral2* that is down-regulated.

Expression of two genes *Fral2* and *TCF15* was verified by *in situ* hybridization (Fig. 7G). In *Hv*_AEP maintained at RT, both genes are predominantly expressed in cells from the epidermal layer, epithelial cells but also neurons sticking to these cells (Supplemental-FigureS1). Consistently, in *Ho_CS* animals maintained at 18°C, we found *Fral2* expressed at high levels in neurons of the apical region and along the body column, and at low levels in epithelial cells, but we did not detect *Fral2*-expressing cells in *Ho_CR* polyps. After 35 days at 10°C, the testes are already post-mature in *Ho_CR* where few *Fral2* expressing cells can be detected (arrowheads). In aging *Ho_CS* where testes are still fully mature, we found *Fral2* predominantly expressed at the base, where spermatogonia are found. *Fral2* transcripts were also detected in some small cells spread along the body column. This result suggests a role for *Fral2* in spermatogenesis as identified in mice (Cohen et al., 1994). Concerning *TCF15* expression, it was undetectable in animals maintained at 18°C, but strong in whole testes (Fig. 7G). These modulations of expression patterns indicate that both genes are up-regulated upon gametogenesis, *Fral2* expression being seemingly shifted from the neuronal lineage to the germ cells in testes.

Discussion

In *Hydra* neurogenesis is constantly active although at a low rate in intact adult animals, replacing the neurons that get sloughed off at the extremities throughout the animal life. After bisection, neurogenesis becomes activated and rapidly re-establishes the apical or basal nervous system in the regenerated structure. In this study, we show that the active behaviors are impaired shortly after aging is induced in *Ho_CS* animals. Indeed, contractility or prey capture behaviors become altered long before the loss of nerve cells or the anatomical disorganization of the nervous system are observed. These alterations, behavioral, anatomical and cellular, are well supported by the molecular analyses. The transcriptomics analysis detects changes in the expression profile of a number of neurotransmission related genes already two weeks after transfer to cold, such as several GABA and glutamate receptors that are down-regulated in both *Ho_CS* and *Ho_CR* animals maintained at 10°C. A recent study claims that the neural circuits that mediate the response to glutathione are located in the hypostome and make use of GABA as neurotransmitter (Lauro and Kass-Simon, 2018). As the down-regulation of the GABA receptor genes is more pronounced in *Ho_CS* than in *Ho_CR*, this difference might explain the lowered ability of *Ho_CS* to capture preys.

The homeoprotein Prdl-a was initially identified as a marker of apical neuronal progenitors with the expected nuclear localization (Gauchat et al., 1998). In aging *Hydra,* i.e. sexual *Ho_CS,* but not in *Ho_CR,* we noticed a striking decrease in the number of prdl-a^{+} cells while the level of *prdl-a* transcripts remained similar between the two strains. After induction of gametogenesis, the number of ISCs rapidly drops in both *Ho_CS* and *Ho_CR* (Yoshida et al., 2006; Tomczyk et al., 2017), but goes back to the homeostatic level in *Ho_CR* while remaining low in *Ho_CS.* The persistence of prdl-a^{+} cells in asexual *Ho_CS* and *Ho_CR* animals maintained at 10°C for 44 days suggest that their loss is connected with the aging process. The *prdl-a* RNA-seq expression profile reflects this transient loss of ISCs and the subsequent recovery in *Ho_CR*. In *Ho_CS* the *prdl-a* RNA-seq expression profile is similar but the ISCs population remains depleted suggesting an ectopic, possibly epithelial, up-regulation of *prdl-a,* although not detected at the protein level. Indeed, we were able to detect such ectopic expression in patches of *prdl-a+* cells along the body column of aging *Ho_CS.* This ectopic up-regulation might be interpreted as an attempt to reactivate neurogenesis in response to the low number of ISCs and neuronal progenitors, but as the epithelial context is not appropriate, the prdl-a protein would not be properly translated or stabilized.

Similarly, the comparative transcriptomic analysis between *Ho_CR* and *Ho_CS* undergoing gametogenesis reflects the intensity of the loss of neurogenesis on the one hand, and the attempt of the aging animals to rescue neurogenesis on the other hand. Indeed, the loss of mature neurons is well visible in *Ho_CS* but not in *Ho_CR* where the number of neuronal progenitors appears unchanged, implying that in *Ho_CR*, *de novo* neurogenesis is maintained at low pace to replace the old neurons. This state is reflected in the global qRNA-seq results with the heatmaps indicating that large sets of neurotransmission and neurogenesis genes are differently down-regulated in *Ho_CR* and *Ho_CS*, mildly and transiently in *Ho_CR,* in a sustained fashion in *Ho_CS*. By contrast, a subset of

neurotransmission and neurogenesis genes show the opposite behavior: strongly up-regulated in *Ho_CS* while rather down-regulated in *Ho_CR*. This second behavior suggests two distinct interpretations: (i) an attempt to rescue neurogenesis in *Ho_CS* by up-regulating a series of key genes for neurogenesis; (ii) the capture of neurogenic genes to the benefice of gametogenesis as shown for *Fral2*.

Among these neurogenesis genes *Otx1, Otx2* or *Gli3* are involved in brain development in mammals, while *Dlx1, Meis1,* and *PUM2* are involved in neuronal survival and differentiation. *Hydra* interstitial cells are able to sense their density and respond to a lower density by increasing their proliferation rate (David et al., 1991). As the number of ISCs and neuronal progenitors strongly decreases in aging *Ho_CS* over the first month, the remaining cells may respond to this low density by over-expressing genes involved in stem cell proliferation and nerve cell differentiation to re-establish the nervous system. This scenario could explain how a large set of genes exhibit similar expression levels between *Ho_CS* and *Ho_CR* despite a dramatically different number of ISCs recorded in these animals when maintained for 35 days at 10°C.

Here we should mention that the loss of ISCs and interstitial cells is actually more massive and definitive after three courses of HU treatment than in *Ho* animals undergoing gametogenesis (Tomczyk et al., 2017; Buzgariu et al., 2018). In fact, in HU-treated *Hv-sf1* the depletion of ISCs and neuronal progenitors is almost complete and leads to the complete loss of expression of numerous neurogenic genes (Wenger et al., 2016). When we compare the molecular consequences of these two types of neurogenesis loss, we identify nine genes up-regulated in aging *Ho_CS* but not at all or to a lower level in the non-aging *Ho_CR*, and at least four-fold in aging *Ho_CS* when compared to HU-treated *Hv_sf1*. For this latter comparison, the results are only indicative as the *Hv* and *Ho* transcriptomes were not generated and processed together, therefore the quantitative approach taken here needs to be confirmed.

Among these genes, we find interestingly *FoxJ3*, initially identified in the neurectoderm of mouse embryos (Landgren and Carlsson, 2004), but also identified as a regulator of spermatogenesis in adult mice (Ni et al. 2016). These genes are either ubiquitously expressed or predominantly expressed in ESCs, suggesting that their up-regulation in aging animals takes place either in epithelial cells or in testes as observed here for *Fral2* and *TCF15* by *in situ* hybridization, an experiment that validates the transcriptomic comparative analysis.

Fra-1 and *Fra-2* are bZIP transcription factors initially identified as stress factors that belong to the Fos-related family (Franza et al., 1988). In mammals, they are essential for development, involved in tumorigenesis of multiple organs and in fibrotic diseases (Eferl and Wagner, 2003; Wernig et al., 2017), with a key regulation by the ERK pathway (Gillies et al., 2017). In *Hydra* where five copies of Fra-like genes are found (Supplementary Figure-S2), *Fral2* expression switches between asexual and sexual animals, from neurons to male germ cells. As the base of testes contains early spermatogonia that actively proliferate to produce sperm cells, this change in *Fral2* expression suggests a recruitment by the germ cells at the expenses of the nerve cells, a competition process possibly leading to aging.

Fral2 could potentially play a cytoprotective function in this highly active cell population. The low epidermal expression of *TCF15* in standard asexual conditions versus the high gonadic expression in aging animals suggests that in sexual *Hydra TCF15* is recruited to play a role in gametogenesis. In mammals TCF15 is a transcription factor implicated in the priming of the pluripotent embryonic stem cells towards differentiation (Davies et al., 2013).

In summary, we demonstrate an aging-dependent loss of the function, density and organization of nervous system in *Hydra*. These adverse changes are caused by a partial loss of ISCs and neuronal progenitors that occurs as a consequence of the intense production of gametes from ISCs. We identify some candidate regulators of this somatic to germinal switch as *Fral2*, pointing to a possible competition for molecular resources between the somatic – neuronal-and germ cell fate of ISCs.

Supplementary Material

Refer to Web version on PubMed Central for supplementary material.

Acknowledgements

The authors thank C. Grimmelikhuijzen (Copenhagen) for kindly providing the anti-RFamide antibody, Y. Wenger for the assistance with the transcriptomic analyses. This work was supported by the Swiss National Science Foundation (SNF grants 31003A_149630, 31003_169930), the National Institute of Health (grant R01AG037962), the Claraz donation and the Canton of Geneva.

References

Alexopoulou Z, Lang J, Perrett RM, Elschami M, Hurry MED, Kim HT, Mazaraki D, Szabo A, Kessler BM, Goldberg AL, Ansorge O, Fulga TA, et al. 2016 Deubiquitinase Usp8 regulates α-synuclein clearance and modifies its toxicity in Lewy body disease. Proc Natl Acad Sci USA 113: E4688–4697. [PubMed: 27444016]

Anderson PA, Spencer AN. 1989 The importance of cnidarian synapses for neurobiology. J Neurobiol 20: 435–57. [PubMed: 2568389]

Baptista MS, Duarte CB, Maciel P. 2012 Role of the ubiquitin-proteasome system in nervous system function and disease: using C. elegans as a dissecting tool. Cell Mol Life Sci 69: 2691–2715. [PubMed: 22382927]

Bode H, Lengfeld T, Hobmayer B, Holstein TW. 2008 Detection of expression patterns in Hydra pattern formation. Methods Mol Biol 469: 69–84 [PubMed: 19109704]

Bode HR, Berking S, David C, Gierer A, Schaller H, Trenker E. 1973 Quantitative analysis of cell types during growth and regeneration in hydra. Roux' Arch Dev Biol 171: 269–285.

Boya P, Codogno P, Rodriguez-Muela N. 2018 Autophagy in stem cells: repair, remodelling and metabolic reprogramming. Development 145: dev146506.

Brien P 1953 La pérennité somatique. Biological Reviews 28: 308–349.

Buzgariu W, Al Haddad S, Tomczyk S, Wenger Y, Galliot B. 2015 Multi-functionality and plasticity characterize epithelial cells in Hydra. Tissue Barriers 3: e1068908. [PubMed: 26716072]

Buzgariu W, Wenger Y, Tcaciuc N, Catunda-Lemos AP, Galliot B. 2018 Impact of cycling cells and cell cycle regulation on Hydra regeneration. Dev Biol 433: 240–253. [PubMed: 29291976]

Campbell RD. 1976 Elimination by Hydra interstitial and nerve cells by means of colchicine. J Cell Sci 21: 1–13. [PubMed: 932105]

Cohen DR, Sinclair AH, McGovern JD. 1994 SRY protein enhances transcription of Fos-related antigen 1 promoter constructs. Proc Natl Acad Sci U S A 91: 4372–4376 [PubMed: 8183916]

Collins AG, Schuchert P, Marques AC, Jankowski T, Medina M, Schierwater B. 2006 Medusozoan phylogeny and character evolution clarified by new large and small subunit rDNA data and an

assessment of the utility of phylogenetic mixture models. Syst Biol 55: 97–115. [PubMed: 16507527]

David CN. 1973 A quantitative method for maceration of hydra tissue. Roux' Arch Dev Biol 171: 259–268.

David CN, Fujisawa T, Bosch TCG. 1991 Interstitial stem cell proliferation in hydra: Evidence for strain-specific regulatory signals. Dev Biol 148: 501–507. [PubMed: 1743398]

Davies OR, Lin CY, Radzisheuskaya A, Zhou X, Taube J, Blin G, Waterhouse A, Smith AJ, and Lowell S 2013 Tcf15 primes pluripotent cells for differentiation. Cell reports 3: 472–484. [PubMed: 23395635]

Dupre C, Yuste R. 2017 Non-overlapping neural networks in Hydra vulgaris. Curr Biol 27:1085–1097. [PubMed: 28366745]

Eferl R, Wagner EF. 2003 AP-1: a double-edged sword in tumorigenesis. Nat Rev Cancer 3: 859–868. [PubMed: 14668816]

Franza BR Jr., Rauscher FJ 3rd, Josephs SF, Curran T 1988 The Fos complex and Fos-related antigens recognize sequence elements that contain AP-1 binding sites. Science 239: 1150–1153. [PubMed: 2964084]

Fujisawa T 1989 Role of interstitial cell migration in generating position-dependent patterns of nerve cell differentiation in Hydra. Dev Biol 133: 77–82. [PubMed: 2707488]

Galliot B, Quiquand M. 2011 A two-step process in the emergence of neurogenesis. Eur J Neurosci 34: 847–862. [PubMed: 21929620]

Galliot B, Quiquand M, Ghila L, Rosa R de, Miljkovic-Licina M, Chera S 2009 Origins of neurogenesis, a cnidarian view. Dev Biol 332: 2–24. [PubMed: 19465018]

Gauchat D, Escriva H, Miljkovic-Licina M, Chera S, Langlois MC, Begue A, Laudet V, Galliot B. 2004 The orphan COUP-TF nuclear receptors are markers for neurogenesis from cnidarians to vertebrates. Dev Biol 275: 104–23. [PubMed: 15464576]

Gauchat D, Kreger S, Holstein T, Galliot B. 1998 prdl-a, a gene marker for hydra apical differentiation related to triploblastic paired-like head-specific genes. Development 125: 1637–45. [PubMed: 9521902]

Gillies TE, Pargett M, Minguet M, Davies AE, Albeck JG. 2017 Linear Integration of ERK Activity Predominates over Persistence Detection in Fra-1 Regulation. Cell Syst 5: 549–563 e545. [PubMed: 29199017]

Grens A, Mason E, Marsh JL, Bode HR. 1995 Evolutionary conservation of a cell fate specification gene: the Hydra achaete-scute homolog has proneural activity in Drosophila. Development 121: 4027–4035. [PubMed: 8575303]

Grimmelikhuijzen CJ. 1985 Antisera to the sequence Arg-Phe-amide visualize neuronal centralization in hydroid polyps. Cell Tissue Res 241: 171–182.

Grimmelikhuijzen CJ, Westfall JA. 1995a The nervous systems of cnidarians. EXS 72: 7–24. [PubMed: 7833621]

Grimmelikhuijzen CJP, Westfall JA. 1995b The nervous systems of Cnidarians. In: Breidbach O, Kutsch W, editors. The Nervous Systems of Invertebrates: An Evolutionary and Comparative Approach, Basel, Switzerland: Birkhaüser Verlag, p 7–24.

Grosvenor W, Rhoads DE, Kass-Simon G. 1996 Chemoreceptive control of feeding processes in hydra. Chem Senses 21: 313–321. [PubMed: 8670710]

Grunder S, Assmann M. 2015 Peptide-gated ion channels and the simple nervous system of Hydra. J Exp Biol 218: 551–561. [PubMed: 25696818]

Hager G, David CN. 1997 Pattern of differentiated nerve cells in hydra is determined by precursor migration. Development 124: 569–576. [PubMed: 9053332]

Hansen GN, Williamson M, Grimmelikhuijzen CJ. 2000 Two-color double-labeling in situ hybridization of whole-mount Hydra using RNA probes for five different Hydra neuropeptide preprohormones: evidence for colocalization. Cell Tissue Res 301: 245–253. [PubMed: 10955720]

Hobmayer B, Jenewein M, Eder D, Eder MK, Glasauer S, Gufler S, Hartl M, Salvenmoser W. 2012 Stemness in Hydra -a current perspective. Int J Dev Biol 56: 509–517. [PubMed: 22689357]

Kass-Simon G, Pierobon P. 2007 Cnidarian chemical neurotransmission, an updated overview. Comp Biochem Physiol A 146: 9–25.

Koizumi O 2007 Nerve ring of the hypostome in hydra: is it an origin of the central nervous system of bilaterian animals? Brain Behav Evol 69: 151–9. [PubMed: 17230023]

Landgren H, Carlsson P. 2004 FoxJ3, a novel mammalian forkhead gene expressed in neuroectoderm, neural crest, and myotome. Dev Dyn 231: 396–401. [PubMed: 15366017]

Lauro BM, Kass-Simon G. 2018 Hydra's feeding response: Effect of GABAB ligands on GSH-induced electrical activity in the hypostome of H. vulgaris. Comp Biochem Physiol, Part A Mol Integr Physiol 225:83–93.

Lichtneckert R, Reichert H. 2009 Origin and Evolution of the First Nervous System. In: Kaas JH, editor. Evolutionary Neuroscience, Oxford: Academic Press -Elsevier, p 51–78.

Loomis WF. 1955 Glutathione control of the specific feeding reactions of hydra. Ann NY Acad Sci 62:209–228.

Marcum BA, Campbell RD. 1978 Development of Hydra lacking nerve and interstitial cells. J Cell Sci 29:17–33. [PubMed: 627604]

Marcum BA, Fujisawa T, Sugiyama T. 1980 A mutant hydra strain (sf-1) containing temperature-sensitive interstitial cells. In: Tardent P, Tardent R, editors. Developmental and Cellular Biology of Coelenterates, Amsterdam: Elsevier/North Holland, p 429–434.

Marlow HQ, Srivastava M, Matus DQ, Rokhsar D, Martindale MQ. 2009 Anatomy and development of the nervous system of Nematostella vectensis, an anthozoan cnidarian. Dev Neurobiol 69: 235–54. [PubMed: 19170043]

Martínez DE 1998 Mortality Patterns Suggest Lack of Senescence in Hydra. Exp Geront 33: 217–225.

Miljkovic-Licina M, Chera S, Ghila L, Galliot B. 2007 Head regeneration in wild-type hydra requires de novo neurogenesis. Development 134: 1191–201. [PubMed: 17301084]

Miljkovic-Licina M, Gauchat D, Galliot B. 2004 Neuronal evolution: analysis of regulatory genes in a first-evolved nervous system, the hydra nervous system. Biosystems 76: 75–87. [PubMed: 15351132]

Mochizuki K, Sano H, Kobayashi S, Nishimiya-Fujisawa C, Fujisawa T. 2000 Expression and evolutionary conservation of nanos-related genes in Hydra. Dev Genes Evol 210: 591–602. [PubMed: 11151296]

Ni L, Xie H, Tan L. 2016 Multiple roles of FOXJ3 in spermatogenesis: A lesson from Foxj3 conditional knockout mouse models. Mol Reprod Dev 83: 1060–1069. [PubMed: 27739607]

Pierobon P 2015 Regional modulation of the response to glutathione in Hydra vulgaris. J Exp Biol 218: 2226–2232. [PubMed: 25987735]

Prochiantz A, Di Nardo AA. 2015 Homeoprotein signaling in the developing and adult nervous system. Neuron 85: 911–925. [PubMed: 25741720]

Richards GS, Simionato E, Perron M, Adamska M, Vervoort M, Degnan BM. 2008 Sponge genes provide new insight into the evolutionary origin of the neurogenic circuit. Curr Biol 18: 1156–1161. [PubMed: 18674909]

Sacks PG, Davis LE. 1979 Production of nerveless Hydra attenuata by hydroxyurea treatments. J Cell Sci 37: 189–203. [PubMed: 479324]

Schaible R, Scheuerlein A, Dańko MJ, Gampe J, Martínez DE, Vaupel JW. 2015 Constant mortality and fertility over age in Hydra. Proc Natl Acad Sci USA 201521002.

Takahashi T, Koizumi O, Ariura Y, Romanovitch A, Bosch TC, Kobayakawa Y, Mohri S, Bode HR, Yum S, Hatta M, Fujisawa T. 2000 A novel neuropeptide, Hym-355, positively regulates neuron differentiation in Hydra. Development 127: 997–1005. [PubMed: 10662639]

Tardent P 1995 The cnidarian cnidocyte, a high-tech cellular weaponry. BioEssays 17: 351–362.

Technau U, Holstein TW. 1996 Phenotypic maturation of neurons and continuous precursor migration in the formation of the peduncle nerve net in Hydra. Dev Biol 177: 599–615. [PubMed: 8806835]

Teragawa CK, Bode HR. 1995 Migrating interstitial cells differentiate into neurons in hydra. Dev Biol 171: 286–293. [PubMed: 7556913]

Tomczyk S, Fischer K, Austad S, Galliot B. 2015 Hydra, a powerful model system for aging studies. Invertebrate Reproduction and Development 59: 11–16. [PubMed: 26120246]

Tomczyk S, Schenkelaars Q, Suknovic N, Wenger Y, Ekundayo K, Buzgariu W, Bauer C, Fisher KE, Austad S, Galliot B. 2017 Deficient autophagy drives aging in Hydra. bioRxiv DOI: 10.110/36638.

Wenger Y, Buzgariu W, Galliot B. 2016 Loss of neurogenesis in Hydra leads to compensatory regulation of neurogenic and neurotransmission genes in epithelial cells. Philos Trans R Soc Lond B Biol Sci 371: 20150040. [PubMed: 26598723]

Wernig G, Chen SY, Cui L, Van Neste C, Tsai JM, Kambham N, Vogel H, Natkunam Y, Gilliland DG, Nolan G et al. 2017 Unifying mechanism for different fibrotic diseases. Proc Natl Acad Sci U S A 114: 4757–4762. [PubMed: 28424250]

Xi Y, Dhaliwal JS, Ceizar M, Vaculik M, Kumar KL, Lagace DC. 2016 Knockout of Atg5 delays the maturation and reduces the survival of adult-generated neurons in the hippocampus. Cell Death & Disease 7: e2127–e2127.

Yoshida K, Fujisawa T, Hwang JS, Ikeo K, Gojobori T. 2006 Degeneration after sexual differentiation in hydra and its relevance to the evolution of aging. Gene 385: 64–70. [PubMed: 17011141]

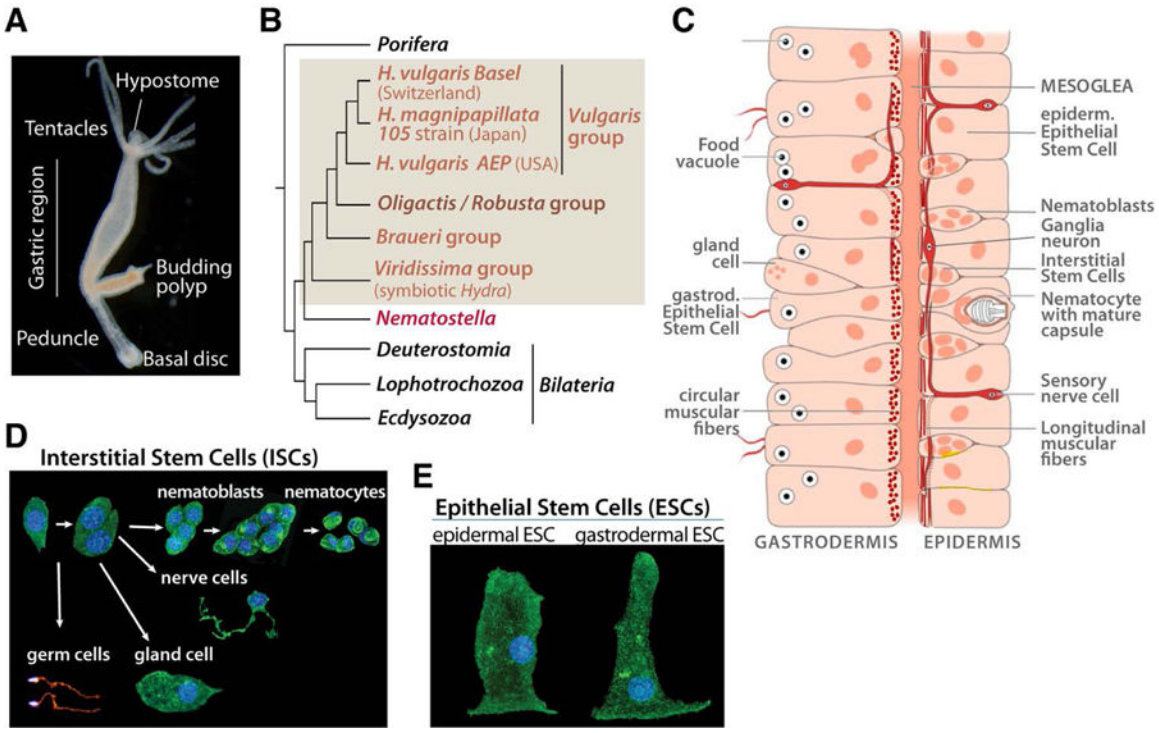

Fig.1. *Hydra* anatomy, phylogenetic position and cell types

(A) Bright field picture of a budding *H. oligactis*. Note the typical stalk shape of the peduncle region. **(B)** Phylogenetic tree showing the respective positions of *H. vulgaris* and *H. oligactis*. **(C)** Schematic view of the bilayered organization of the body column with the gastrodermis (or gut) on the left side and the epidermis on the right one, separated by an acellular matrix named mesoglea. Epithelial cells from both layers contain myofibrils, circular in gESCs and longitudinal in eESCs. Nematoblasts and nematocytes are restricted to the epidermis while nerve cells are present in both layers although more abundant in the outer one. Scheme modified from (Lenhoff and Lenhoff, 1988). **(D, E)** Identification of the various *Hydra* cell types, as observed after tissue maceration followed by b-tubulin immunodetection and DAPI counter staining. Among the derivatives of the multipotent ISCs (D), note the precursors to nematocytes (or cnidocytes) named nematoblasts that divide syncitially before entering differentiation, and the different types of nerve cells: sensory, sensory/motor (bipolar) or ganglion neurons (multipolar). The ESCs (E) are unusual stem cells, i.e. self-renewing and differentiated (Buzgariu et al., 2015).

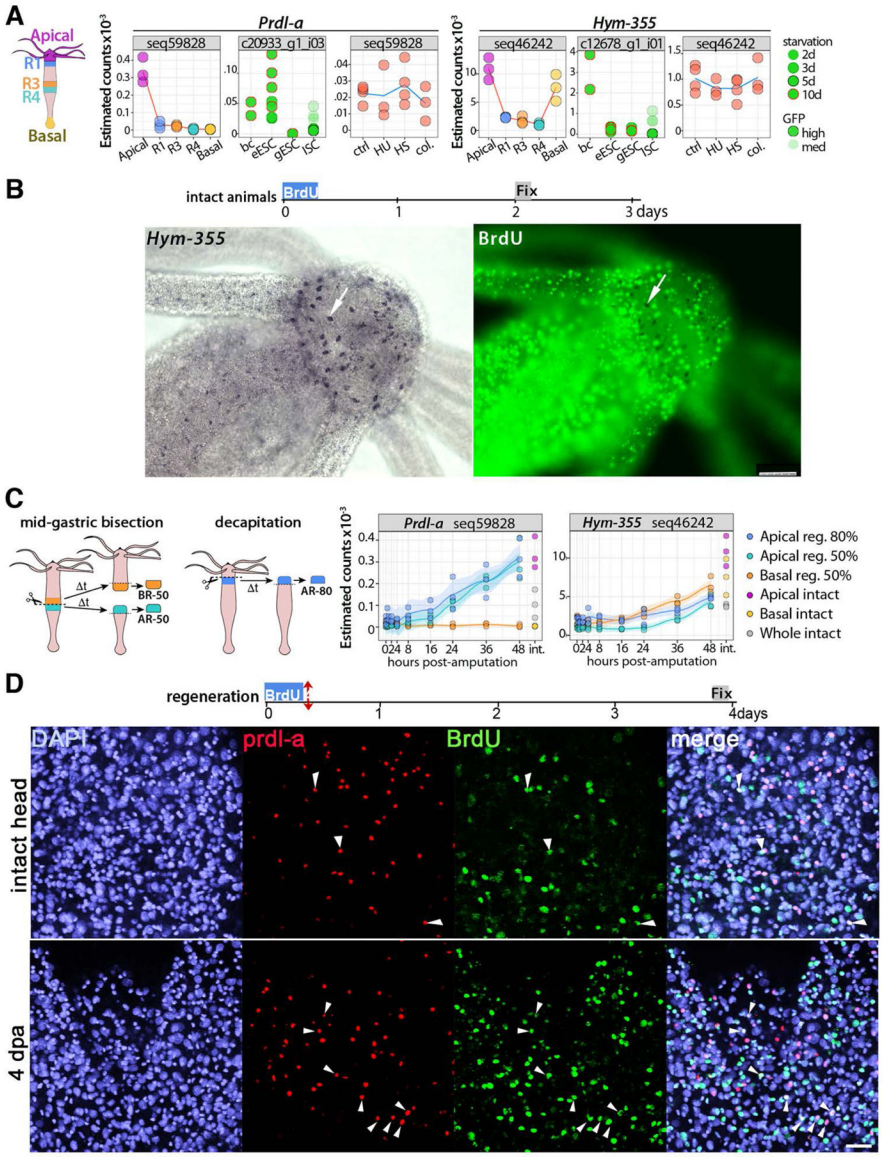

Fig.2. Homeostatic and regeneration-induced *de novo* neurogenesis in slow aging *Hydra vulgaris*.

(A) Expression profiles of the neurogenic genes *Prdl-a* and *Hym-355* as detected in animals of the heat-sensitive *Hv_sf-1* strain through three different RNA-seq approaches performed (a) on tissues from slices of the body column when distinct regions (Head, R1, R3, R4, Foot) were dissected before RNA extraction (see the scheme on the left that indicates the five regions); (b) on distinct cell types, i.e. ectodermal epithelial stem cells (eESC), gastrodermal epithelial stem cells (gESC) and interstitial stem cells (ISCs) isolated by flow-cytometry; (c) on the central body column of animals exposed to drugs (HU, colchicine) or Heat-shock (HS). All transcriptomic procedures are described in (Wenger et al., 2016). **(B)** Lack of $BrdU^{+}$ neurons expressing *Hym-355* in animals exposed to BrdU for four hours and fixed four days later. Scale bar: 25 μm (left) and 75 μm (right). **(C)** Expression profiles of *Prdl-a* and *Hym-355* transcripts detected by RNA-seq in regenerating-tips dissected at various time points of head or foot regeneration. Animals were either bisected at mid-gastric level (50%)

or decapitated (80%). **(D)** Prdl-a (red) and BrdU (green) co-detection in the apex of intact (upper panel) or head-regenerating (lower panel) *H. vulgaris* animals. All animals were exposed to a four hours BrdU pulse, then immediately bisected at mid-gastric level and fixed three days later. In the apical region shown here prdl-a expression is nuclear, enhanced in regenerating heads (Gauchat et al., 1998). The prdl-a^+ and prdl-a^+/$BrdU^+$ cells (white arrowheads) are rare in heads of intact animals but numerous in newly regenerated heads. Scale bar: 25 μm.

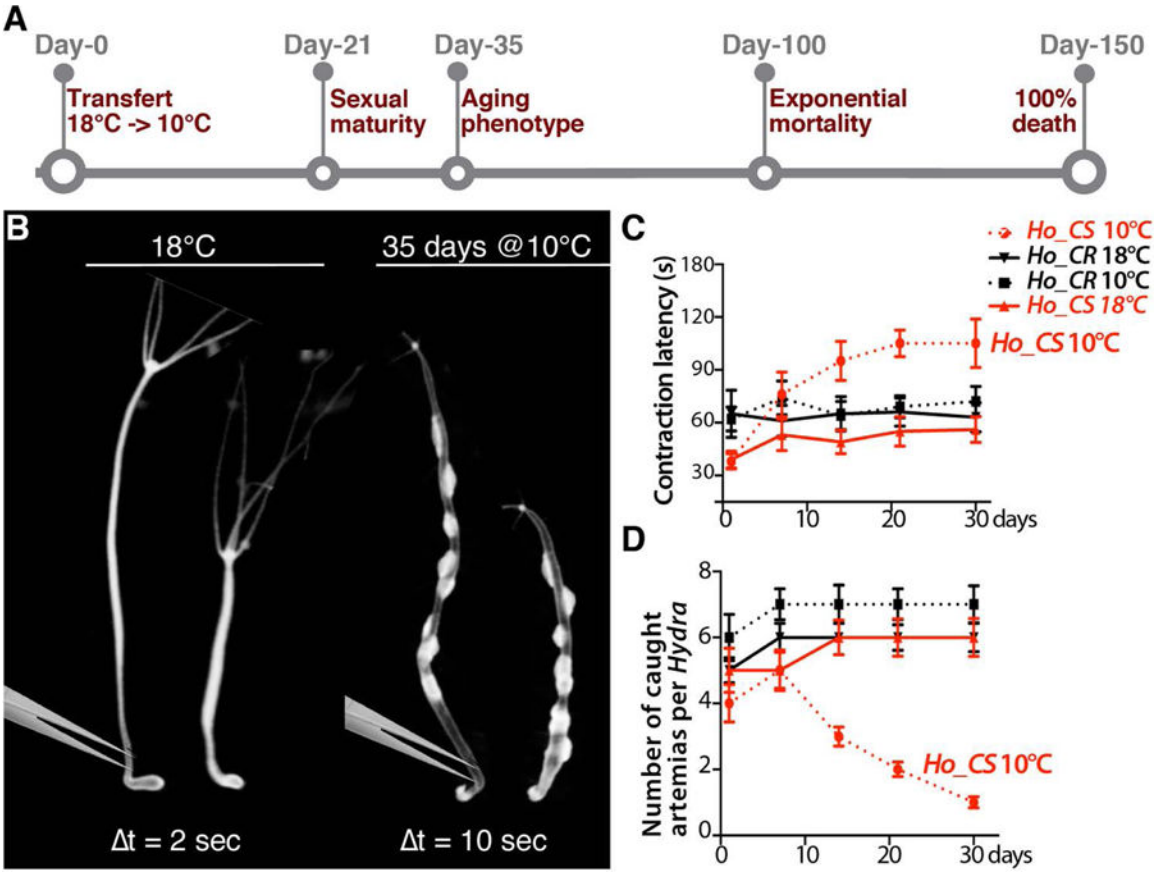

Fig.3. Behavioral alterations in *H. oligactis* animals undergoing aging

(A) Schematic view of the aging process induced in sexual *H. oligactis* cold-sensitive (*Ho_CS*) animals that undergo gametogenesis upon transfer to cold (10°C). Animals from the closely related *H. oligactis* cold-resistant strain (*Ho_CR)* also undergo gametogenesis within three weeks but do not exhibit any aging phenotype and remain fit over the following months (Tomczyk et al., 2017). **(B)** Contractility upon mechanical stimulation in *Ho_CS* animals maintained either at 18°C or at 10°C for 35 days. The contractility in response to tweezer stimulation of the peduncle region was recorded on live animals imaged with an Olympus SZX10 microscope equipped with a DP73 camera (movie). Contraction of the whole animal body takes place within two seconds in animals maintained at 18°C and within 10 seconds in *Ho_CS* animals maintained at 10°C for 35 days. **(C)** Light-induced contractility of *Ho_CS* and *Ho_CR* animals maintained at 10°C (n=15). The contractility was deduced from the time taken by the animal to elaborate a typical contraction response to a bright, directly focused light source. **(D)** Prey capture of *Ho_CS* and *Ho_CR* animals maintained at 10°C (n=15) assessed from the number of *Artemia* fixed on tentacles of each animal normalized by tentacle number. In C and D, the legend codes are the same and the error bars correspond to standard error of the mean (SEM). Note that already two weeks after transfer to 10°C, *Ho_CS* but not *Ho_CR* animals show an extended contraction latency after light exposure and lose the ability to capture preys.

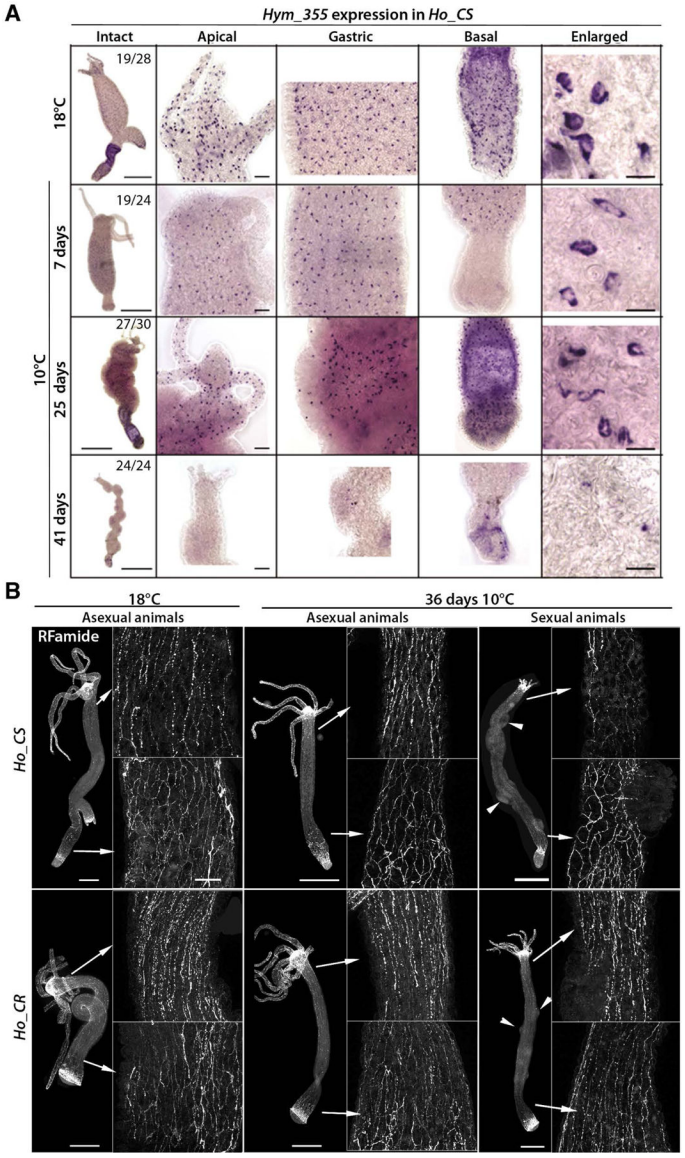

Fig. 4. Loss of neuronal density in *Ho_CS* animals undergoing aging

(A) *Hym-355* expressing nerve cells detected by *in situ* hybridization along the body column of *Ho_CS* animals maintained at 18°C or 10°C for 7, 25 or 41 days. Scale bars: 500 μm (intact), 50 μm (apical, gastric, basal), 10 μm (enlarged). **(B)** RFamide expressing nerve cells immunodetected in *Ho_CS* and *Ho_CR* animals maintained at 18°C or 10°C for 36 days. Arrowheads indicate mature or post-mature testes. Scale bars: 100 μm.

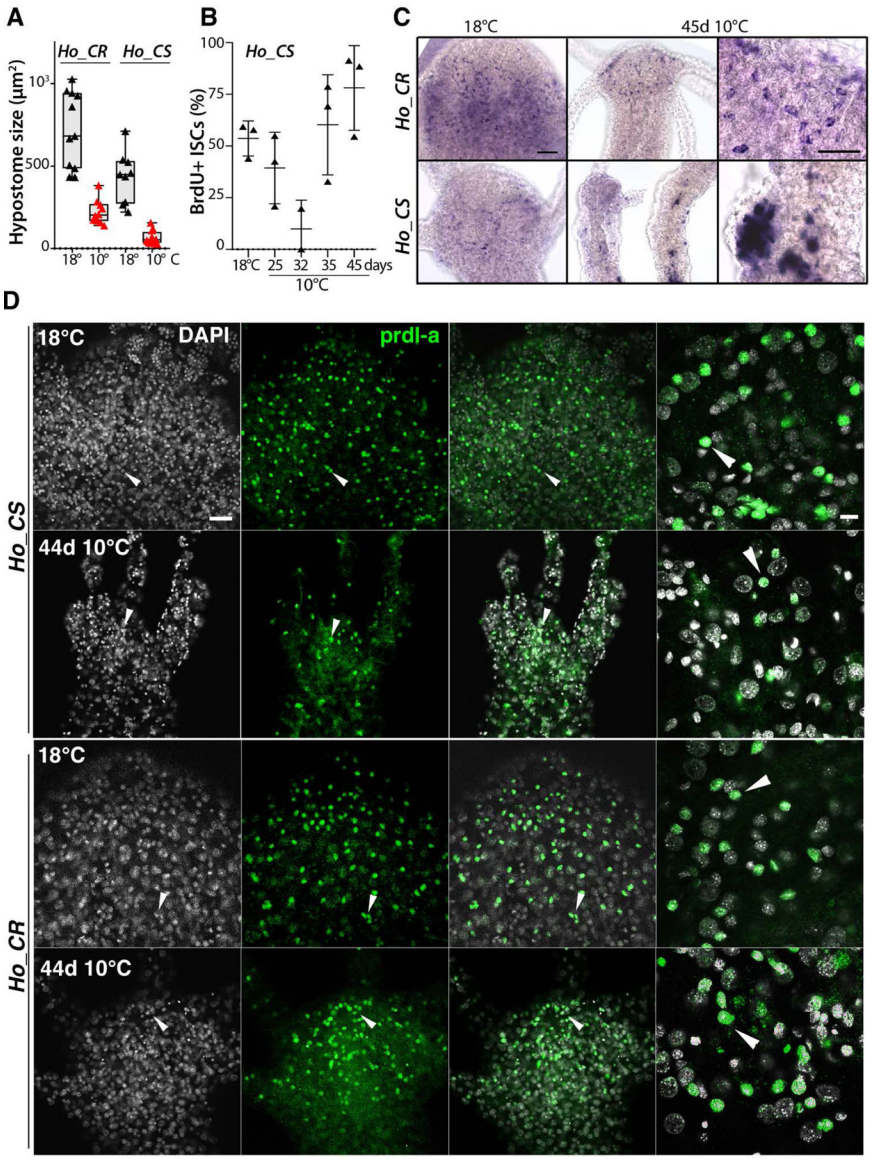

Fig. 5. Loss of neuronal progenitors and *prdl-a*/prdl-a expression in aging *H. oligactis*

(A) Decrease in hypostome size in *Ho_CS* and *Ho_CR* animals maintained at 18°C or 10°C for 35 days. **(B)** Transient decrease in interstitial cycling cells in *Ho_CS*. **(C)** Apical expression of *prdl-a* in *Ho_CS* and *Ho_CR* animals maintained at 18°C or 10°C for 45 days. **(D)** Immunodetection of the homeoprotein prdl-a in *Ho_CS* and *Ho_CR* animals maintained at 18°C or taken 44 days after transfer to 10°C. Scale bars: 20 µm (left panels), 10 µm (right panels). Note the progressive decrease in the number of prdl-a expressing cells in aging *Ho_CS* when compared to *Ho_CR* maintained in the same conditions.

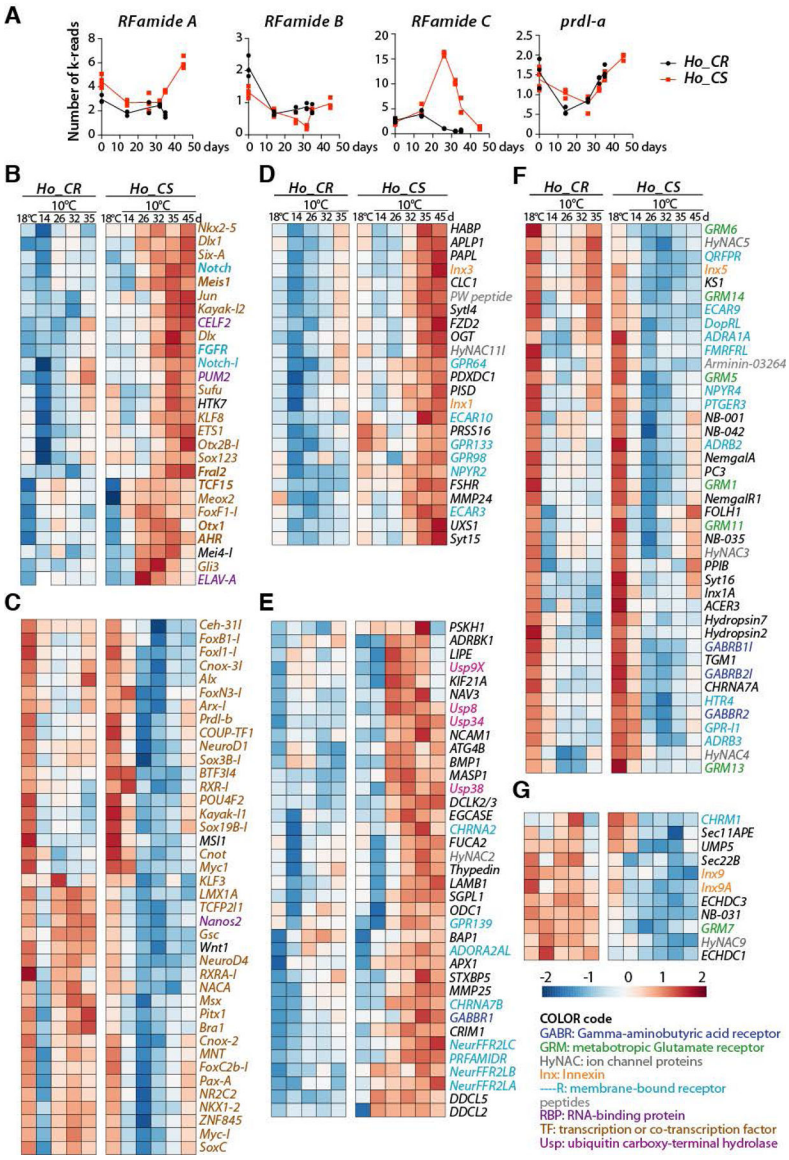

Fig. 6. Modulations of neurogenesis and neurotransmission gene expression in *Ho_CS* and *Ho_CR* animals maintained at 18°C or 10°C.

(A) Expression profiles of the genes encoding the *RFamide* neuropeptides and the *prdl-a* homeoprotein measured by qRNA-seq in *Ho_CR* (blue) and *Ho_CS* (red) animals at indicated time points after transfer to 10°C. **(B-G)** Heatmaps showing the relative expression of 67 genes known or expected to regulate neurogenesis (B, C), and 114 genes whose products are predicted to be involved in neurotransmission (D-G) in *Ho_CR* and *Ho_CS* animals transferred to 10°C at day-0. In panels B, D, E, genes are up-regulated in aging *Ho_CS* animals, while in panels C, F, G, genes are either up-regulated in *Ho_CR* or down-regulated in *Ho_CS*. Sequences from *Hv* orthologs can be found in Table-S1 from Wenger et al. (2016), expression profiles of neurogenesis genes are shown in Supplementary Figure-S1. All expression profiles are accessible at www.hydratlas.unige.ch for *Hv* sequences, at http://129.194.56.90/blast/ for *Ho_CS* and *Ho_CR* ones after tblastn with *Hv* sequences.

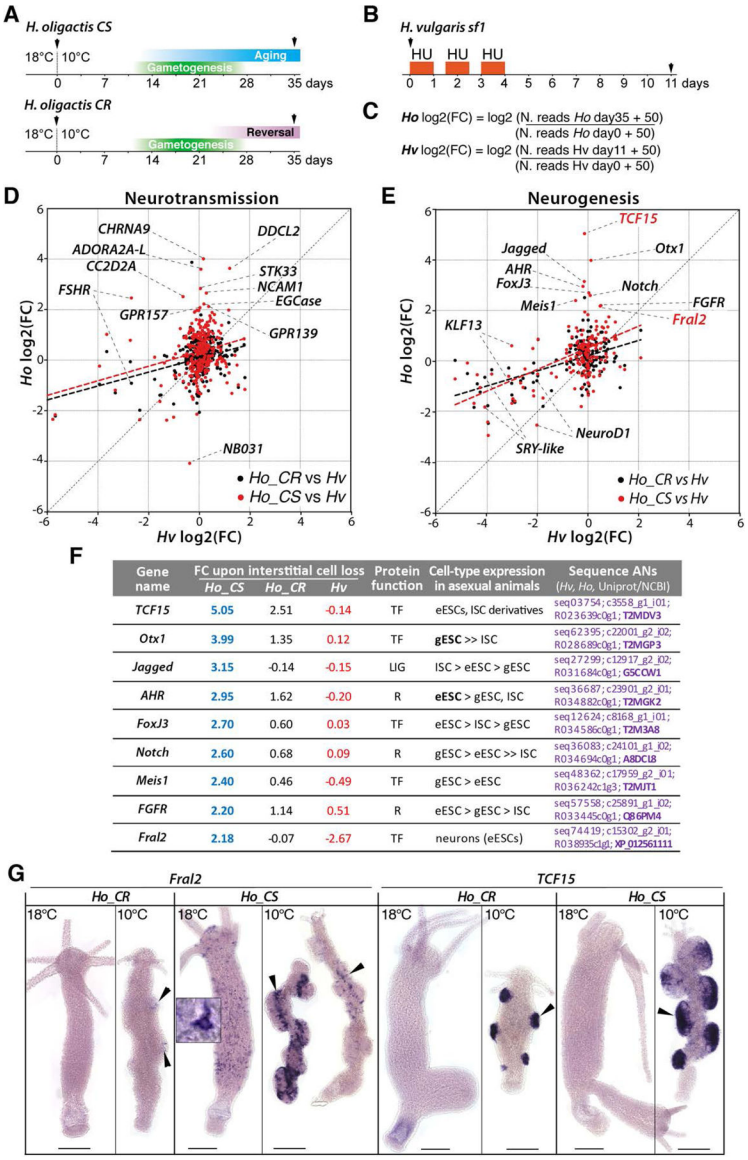

Gene name	FC upon interstitial cell loss			Protein function	Cell-type expression in asexual animals	Sequence ANs (*Hv, Ho*, Uniprot/NCBI)
	Ho_CS	*Ho_CR*	*Hv*			
TCF15	5.05	2.51	-0.14	TF	eESCs, ISC derivatives	seq03754; c3558_g1_i01; R023639c0g1; **T2MDV3**
Otx1	3.99	1.35	0.12	TF	**gESC** >> ISC	seq62395; c22001_g2_i02; R028689c0g1; **T2MGP3**
Jagged	3.15	-0.14	-0.15	LIG	ISC > eESC > gESC	seq27299; c12917_g2_i02; R031684c0g1; **G5CCW1**
AHR	2.95	1.62	-0.20	R	**eESC** > gESC, ISC	seq36687; c23901_g2_i01; R034882c0g1; **T2MGK2**
FoxJ3	2.70	0.60	0.03	TF	eESC > ISC > gESC	seq12624; c8168_g1_i01; R034586c0g1; **T2M3A8**
Notch	2.60	0.68	0.09	R	gESC > eESC >> ISC	seq36083; c24101_g1_i02; R034694c0g1; **A8DCL8**
Meis1	2.40	0.46	-0.49	TF	gESC > eESC	seq48362; c17959_g2_i01; R036242c1g3; **T2MJT1**
FGFR	2.20	1.14	0.51	R	eESC > gESC > ISC	seq57558; c25891_g1_i02; R033445c0g1; **Q86PM4**
Fral2	2.18	-0.07	-2.67	TF	neurons (eESCs)	seq74419; c15302_g2_i01; R038935c1g1; **XP_012561111**

Fig. 7. Comparative analysis of gene modulations of neurotransmission and neurogenesis genes in nerve free *H. vulgaris*, *Ho_CS* and *Ho_CR*.

(A, B) Schemes representing the experimental conditions to produce qRNA-seq data (black arrowheads) from *Ho_CS* and *Ho_CR* animals maintained at 10°C for 35 days, or from *Hv_sf1* animals exposed to hydroxyurea (HU). **(C)** Equations used to calculate the log2 fold change (FC) for *Ho_CS, Ho_CR* animals between day-0 and day-35 of cold exposure, and *Hv_sf1* animals between day-0 and day-11 after HU exposure. **(D, E)** Scatterplot of FC values from *Hv_sf1* (x axis) and *Ho_CS* or *Ho_CR* (y axis). The thick dashed lines represent linear regression for the *Ho_CS* (red), *Ho_CR* (black) conditions. **(F)** Modulations in the expression of nine neurogenic candidate genes in *Ho_CS* and *Ho_CR* animals maintained at 10°C for 35 days (blue and black numbers respectively) and in HU-treated *H. vulgaris* (red numbers) as identified in (E). Fold change values (FC) measured in *Ho_CS* and *Ho_CR* animals maintained at 10°C for 35 days or in HU-treated *Hv_sf1* animals were normalized over the values measured in *Ho* animals maintained at 18°C or in untreated *Hv* animals

respectively. LIG: ligand; R: receptor, TF: transcription factor. Detailed expression profiles are shown in Supplementary Figure-S1. **(G)** Expression patterns of *Fral2* and *TCF15* in *Ho_CS* and *Ho_CR* animals maintained at 18°C or at 10°C for 35 days. Scale bar: 200 μm.